

Strengthening of Fe₃Al Aluminides by One or Two Solute Elements



PETR KRATOCHVÍL, STANISLAV DANIŠ, PETER MINÁRIK, JOSEF PEŠIČKA,
and ROBERT KRÁL

The compressive yield stress of Fe-26Al with additives Ti (0.5 to 4 at. pct), Cr (0.5 to 8 at. pct), Mo (0.5 to 4 at. pct), and V (0.5 to 8 at. pct) at 1073 K (800 °C) has been determined. The effect of the concentration of diverse solutes on the yield stress at 1073 K (800 °C) was compared, and the additivity of the effects of solutes was tested. The effects in iron aluminides with two solutes (V and Ti, Ti and Cr, V and Cr) are compared with those of a single solute V, Ti, and Cr. It is found that the additivity of yield stress increments is valid only for lower solute concentrations. When the amount of the solute atoms increases, the yield stress increment is substantially higher than the sum of the yield stress increments of single solutes. This behavior is related to the high-temperature order in iron aluminides.

DOI: 10.1007/s11661-017-4211-x

© The Minerals, Metals & Materials Society and ASM International 2017

I. INTRODUCTION

ALLOYS based on iron aluminides Fe₃Al show potential for structural applications at high temperatures owing to their excellent oxidation and sulfidation resistance. They display lower density compared to other iron-based materials, and their low cost is advantageous as well. Unfortunately, they also show unfavorable lack of room temperature ductility and low high-temperature strength.^[1–5]

During the last decades, research efforts have focused on enhancing the ductility, strength, and creep resistance of iron aluminides by alloying. Several approaches have been explored to improve the high-temperature mechanical properties of these alloys. Basically, solid solution hardening (SSH), strengthening by coherent and incoherent precipitates, and increasing the crystallographic order were considered for the strengthening of iron aluminides.^[1,6–9] Elements such as Cr, Ti, Mn, Si, Mo, V, and Ni were added for SSH^[2,10–12] and Palm^[8] compared the SSH by Ti, V, Cr, and Mo at 873 K, 973 K, and 1073 K (600°C, 700°C, and 800 °C). Recently, Kratochvil *et al.*^[12] described the SSH effect of

vanadium in Fe₃Al using the SSH theories for binary alloys of Fleischer^[13] and Labusch.^[14] It was reported that the SSH of Fe₃Al by vanadium depends mostly on the elastic modulus misfit, and the atom size misfit plays a minor role.

In this work, we first describe the SSH of Fe₃Al by Ti, Cr, V, and Mo solutes. This is followed by the study of the combined effect of two solutes in Fe₃Al.

II. EXPERIMENTAL

Iron aluminide alloys were produced by vacuum induction melting. The cooling took place under argon. Samples were prepared from the alloys by electrical discharge machining (EDM). The compressive yield stress was evaluated using a digitally controlled testing machine (INSTRON 1186R). Parallelepipeds with dimensions of 6 × 6 × 10 mm³ were cut by EDM. The deformation rate was 8 × 10⁻⁵ s⁻¹. The temperature of 1073 K (800 °C) was chosen because this temperature is well above the yield strength anomaly, which is an unusual increase of the strength with increasing temperature, typically observed for Fe-Al-based alloys with the maximum in the 773 to 873 K (500 to 600 °C) range.^[15] Additionally, 1073 K (800 °C) is high enough for the vacancy concentration to be in thermal equilibrium. This is noteworthy because at lower temperatures the strength of Fe-Al-based alloys is markedly influenced by quenched-in thermal vacancies,^[16] *i.e.*, the strength depends on the processing of the alloys. The investigated alloys are B2-ordered at 1073 K (800 °C), allowing direct comparison of their yield strengths.

PETR KRATOCHVÍL, PETER MINÁRIK, JOSEF PEŠIČKA, and ROBERT KRÁL are with the Charles University, Faculty of Mathematics and Physics, Department of Physics of Materials, Ke Karlovu 5, Prague 2, CZ-12116, Czech Republic. Contact e-mail: pektrat@met.mff.cuni.cz STANISLAV DANIŠ is with the Charles University, Faculty of Mathematics and Physics, Department of Condensed Matter Physics, Ke Karlovu 5, Prague 2, CZ-12116, Czech Republic.

Manuscript submitted June 3, 2017.

Article published online July 6, 2017

Table I. Analyzed Compositions of the Single Solute Alloys (At. Pct)

	Ti		Cr		Mo		V
FA-Ti 0.5	0.62	FA-Cr 0.5	0.66	FA-Mo 0.5	0.56	FA-V 0.5 ^[12]	0.61
FA-Ti 1	1.11	FA-Cr 1	2.24	FA-Mo 2	1.87	FA-V 2 ^[12]	2.22
FA-Ti 2	2.17	FA-Cr 2	4.28	FA-Mo 4	4.00	FA-V 4 ^[12]	4.29
FA-Ti 4	4.17	FA-Cr 5	5.34			FA-V 8	8.55
		FA-Cr 8	8.11				

Table II. Experimentally Determined Yield Stress $\sigma_{0.2}$ (MPa) at 1073 K (800 °C)

	$\sigma_{0.2}$		$\sigma_{0.2}$		$\sigma_{0.2}$		$\sigma_{0.2}$
Ti 0.5	38	Cr 0.5	25.3	Mo 0.5	53.4	V 0.5 ^[12]	57 ^[12]
Ti 1	55	Cr 1	26.9	Mo 2	88.7	V 2 ^[12]	89 ^[12]
Ti 2	73	Cr 2	27.6	Mo 4	102.0	V 4 ^[12]	112 ^[12]
Ti 4	121	Cr 5	30.5			V 8	140
		Cr 8	32.8				

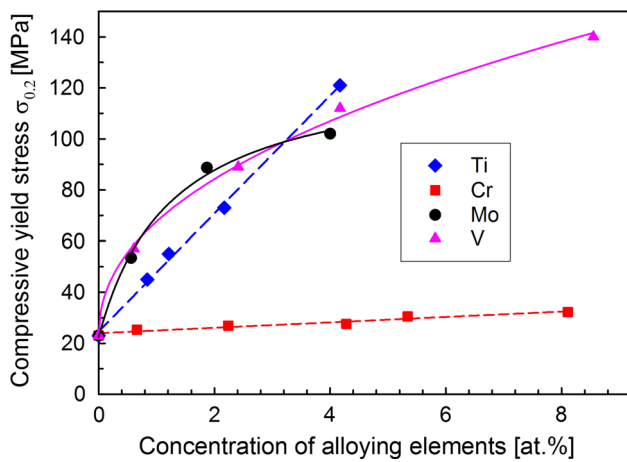


Fig. 1—Dependence of the compressive yield stress $\sigma_{0.2}$ at 1073 K (800 °C) on the concentration of Cr, Ti, Mo, and V.

To reveal the structure of the investigated materials at elevated temperatures, X-ray diffraction measurements at high temperatures were performed. Powdered samples were placed into an AlN crucible and heated up to 1073 K (800 °C) using a radiant heater in vacuum. A high-temperature chamber MRI TC-Basics was placed onto a goniometer of the Panalytical X'Pert MPD diffractometer in the Bragg-Brentano geometry. CuK α radiation was used, and diffracted rays were detected using a gas-filled proportional detector equipped with a graphite monochromator. A constant irradiated area of 3 \times 5 mm² was held during the measurements using automatic divergence slits.

The X-ray study of the microstructure was complemented by transmission electron microscope (TEM) observations. Slices about 0.5 mm thick were cut from the bulk material (as-cast state). These were further ground to the thickness of about 0.1 mm and electro-polished under 15 V at -30 °C (243 K) in 20 pct solution of nitric acid (HNO₃) in methyl alcohol (CH₃OH) to prepare TEM specimens. TEM

observations were performed on JEOL 2000FX working at 200 kV.

III. RESULTS AND DISCUSSION

A. Experiments with Single Solutes

The compositions of the tested alloys were determined by wet chemical analysis (Table I). These alloys show comparable Al content (25.5 ± 0.3 at. pct) and are denoted FA. The C content (0.03 at. pct) is so low that it has no noticeable effect on the yield strength. All alloys are single-phase at room temperature and exhibit a polygonal grain structure with large grains, with sizes between 150 and 500 μ m.

First, the influence of Mo, Ti, Cr, V solutes on the increase of the yield stress $\sigma_{0.2}$ at 1073 K (800 °C) was determined. The values for these ternary alloys are summarized in Table II. The dependencies can be described as functions of c^n (Figure 1). In the case of Cr and Ti, n is equal to 1. For vanadium, $n = 1/2$ was obtained.^[12]

B. Experiments with Two Solutes in Fe₃Al

The investigation of a combined effect of two solutes on the hardening of Fe₃Al (quaternary alloy) was the next step. The compositions were determined by wet chemical analysis of seven tested alloys and are presented in Table III. The structure of all alloys at 1073 K (800 °C)—the testing temperature—was determined by XRD of powder samples (Figure 2). The data for the 3 alloys investigated by Stein *et al.*^[17] are added in Table V. Nominal compositions are listed for these 3 alloys in Table IV.

It is obvious that the combination of two solutes Ti and V, and as well of Cr and V, increases the transformation temperature D0₃→B2 to the temperatures higher than 1073 K (800 °C). In addition to X-ray diffraction, the structure of the Fe₃Al-10V-10Cr alloy was also investigated by TEM (Figure 3). The TEM

Table III. Compositions of Alloys with Two Solutes (At. Pct)

Alloy	Ti	V	Cr
Fe ₃ Al-2Ti-2V	1.99	2.04	
Fe ₃ Al-4Ti-2V (nominal) ^[17]	4	2	
Fe ₃ Al-4Ti-4V	4.02	4.02	
Fe ₃ Al-8Ti-8V	8.00	8.02	
Fe ₃ Al-10Ti-10V	9.78	9.34	
Fe ₃ Al-10V-10Cr		10.2	9.7

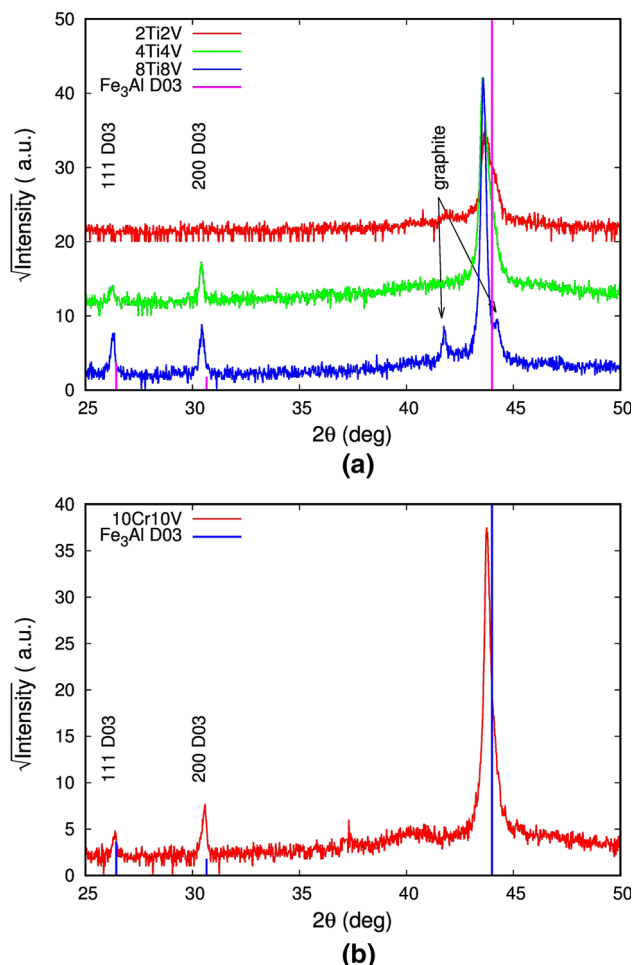


Fig. 2—XRD patterns of tested alloys obtained at 1073 K (800 °C) (a) for three alloys with two solutes Ti-V and (b) one alloy with two solutes Cr-V.

observations are in an agreement with the X-ray results and confirm that the structure is ordered, with a D0₃ symmetry (Figure 3(a)). Ordering in this material is also documented by the presence of both types of anti-phase boundaries (APB) (Figure 3(b)).

Then, the values of the yield stress $\sigma_{0.2}$ at 1073 K (800 °C) in the quaternary systems (Fe₃Al-Cr-V and Fe₃Al-Ti-V) are compared to the corresponding values of the ternary alloys, *i.e.*, the yield stress $\sigma_{0.2}$ of quaternary Fe₃Al-xTi-yV is compared to the sum of individual contributions of Ti and V to the yield stress $\sigma_{0.2}$ determined for ternary alloys Fe₃Al-xTi and Fe₃Al-yV.

The measured values of $\sigma_{0.2}$ for alloys with two solutes in Fe₃Al at 1073 K (800 °C) are given in Table V (column 1). These values are compared to the sum of the measured yield stress $\sigma_{0.2}$ at 1073 K (800 °C) for Fe₃Al-xTi and of the increment yield stress $\Delta\sigma_{0.2}$ at 1073 K (800 °C) for Fe₃Al-xV. The increment of the yield stress $\Delta\sigma_{0.2}$ is equal to the value of the yield stress $\sigma_{0.2}$ for Fe₃Al-xV lowered by the value of the yield stress $\sigma_{0.2}$ of the matrix Fe₃Al that is approximately 23 MPa.^[12] The data presented in the third and fourth columns of Table V as $\sigma_{0.2}$ exp and $\Delta\sigma_{0.2}$ exp, respectively, are interpolated or extrapolated from the dependencies shown in Figure 1 for the value of the respective concentration *c*.

It is found that for low values of *x* and *y* up to ~2 to 4 at. pct, the values $\sigma_{0.2}$ at 1073 K (800 °C) of the quaternary alloys Fe₃Al-xTi-yV are the same as the sums of the respective $\sigma_{0.2}$ exp and $\Delta\sigma_{0.2}$ exp of the ternary alloys. This is also true for the quaternary system Fe-Al-Cr-V.

The value of $\sigma_{0.2}$ at 1073 K (800 °C) for Fe-26Al-4Ti-2V given in Reference 17 (~190 MPa) is similar to that measured in this work (compare line two in Table V). In the same paper,^[17] the value of $\sigma_{0.2}$ at 1073 K (800 °C) for Fe-26Al-4Ti-2Cr is given as ~120 MPa. This is very close to the value of $\sigma_{0.2}$ at 1073 K (800 °C) for Fe-26Al-4Ti (see Table II and Figure 1) owing to the very small $\Delta\sigma_{0.2}$ contributed by Cr (for Fe₃Al-2Cr it is 2 to 5 MPa).

This is true unless the concentration is increased over a certain, not yet determined limit. The structure of the Fe₃Al-4 at. pct Ti-4 at. pct V and Fe₃Al-8 at. pct Ti-8 at. pct V alloys is D0₃-(L2₁-) ordered at 1073 K (800 °C), as shown in Figure 2(a). The diffraction curves at 1123 K, 1223 K, and 1323 K (850 °C, 950 °C, and 1050 °C) are available for Fe₃Al-8 at. pct Ti-8 at. pct V and show a D0₃ (L2₁) order, in agreement with the phase transformation at 1423 K (1150 °C) detected by DTA.^[18]

The same situation is observed for the alloy Fe₃Al-10 at. pct Cr-10 at. pct V. The additivity of the yield stresses 0.2 at 1073 K (800 °C) is no longer valid. The increased strengthening effect can also here be connected with D0₃ (L2₁) order (see Figure 2(b)). The ordering effect of each of V and Cr (*i.e.*, the effect on increase of D0₃↔B2 temperature in iron aluminide Fe₃Al), by 1 to 4 at. pct of both elements, was described by Anthony and Fultz.^[19] The effect of Ti on D0₃ order was also studied in detail in References 20 and 21. Very recently, the Fe₃Al iron aluminides substantially alloyed with Ti

(generating coherent A2 + L₂₁ microstructure) were used for near-net-shape processing technologies.^[22]

IV. CONCLUSION

The main task of describing the rules of the cooperative hardening of Fe₃Al by two solutes can be divided into two parts:

Table IV. Nominal Compositions of Alloys (At. Pct) in Ref. [17]

Alloys, Ref. [17]	Ti	V	Cr, Mo
Fe ₃ Al-4Ti-2Cr	4		2 Cr
Fe ₃ Al-4Ti-2V	4	2	
Fe ₃ Al-4Ti-2Mo	4		2 Mo

1. It is obvious that for dilute alloys, the addition of hardening by individual solutes describes the real properties of the alloys. This can be seen in the data presented in Table V for the first two and last three alloys—the addition of $\sigma_{0.2 \text{ exp}}$ and $\Delta\sigma_{0.2 \text{ exp}}$.
2. For a further increase of concentration of both solutes, the strength $\sigma_{0.2 \text{ exp}}$ of the alloys is greater than the sum of $\sigma_{0.2 \text{ exp}}$ and $\Delta\sigma_{0.2 \text{ exp}}$. This increase is due to the structure of the tested alloys at 1073 K (800 °C), *i.e.*, to the D0₃ (L₂₁) order of alloys Fe₃Al-4Ti-4V, Fe₃Al-8Ti-8V, and Fe₃Al-10V-10Cr.

In further research, the iron aluminide Fe₃Al will be used for studies of a series of multicomponent alloys. These studies will aim to determine how far the good anticorrosion properties of iron aluminides can be maintained in Fe₃Al containing high concentrations of two or more solutes.

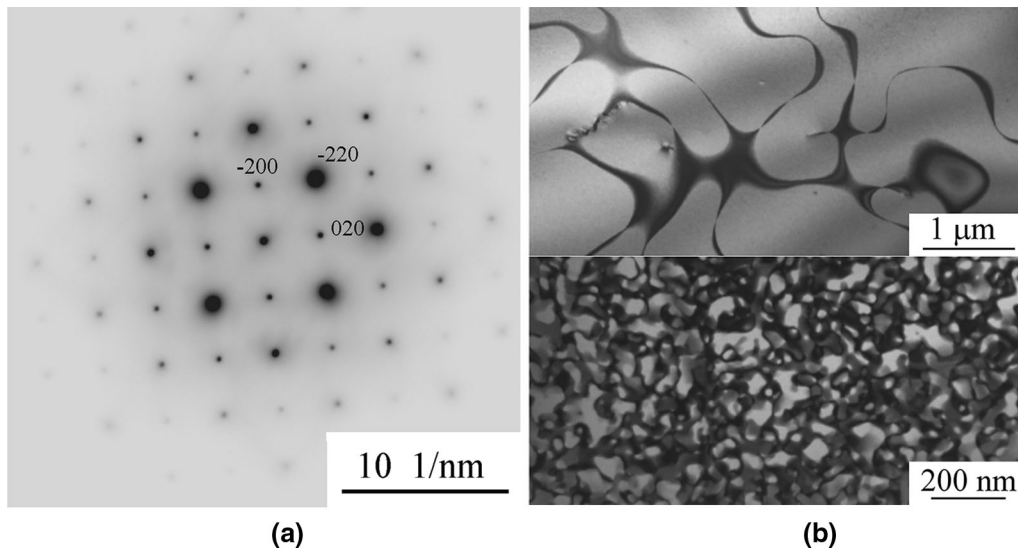


Fig. 3—Selected area diffraction pattern, pole [001] (a). Imaging of APB 1 (displacement vector $a/4 \langle 111 \rangle$) using $g = \langle 200 \rangle$ (upper part) and APB 2 (displacement vector $a/2 \langle 100 \rangle$) using $g = \langle 111 \rangle$ (lower part) of (b).

Table V. Yield Stresses (MPa)

Alloy	$\sigma_{0.2 \text{ exp}}$	$\sigma_{0.2 \text{ exp Fe}_3\text{Al-xTi}$	$\Delta\sigma_{0.2 \text{ exp Fe}_3\text{Al-xV}$	Sum
Fe ₃ Al-2Ti-2V	113	71	60	131
Fe ₃ Al-4Ti-2V	177	117	60	176
Fe ₃ Al-4Ti-4V	222	117	83	200
Fe ₃ Al-8Ti-8V	405	207	115	322
Fe ₃ Al-10Ti-10V	648	340	120	460
Fe ₃ Al-10V-10Cr	234	$\sigma_{0.2 \text{ exp Fe}_3\text{Al-xV}$ 155	$\Delta\sigma_{0.2 \text{ exp Fe}_3\text{Al-yCr}$ 10	165
Alloy Ref. [17]		$\sigma_{0.2 \text{ exp Fe}_3\text{Al-4Ti}$	$\Delta\sigma_{0.2 \text{ exp Fe}_3\text{Al-Cr,V,Mo}$	
Fe ₃ Al-4Ti-2Cr	120	117	4	121
Fe ₃ Al-4Ti-2V	190	117	60	177
Fe ₃ Al-4Ti-2Mo	190	117	60	177

ACKNOWLEDGMENTS

Most of the alloys used in this work were kindly prepared by Frank Stein and Johannes Deges of the MPI für Eisenforschung in Düsseldorf, Germany. This help is acknowledged. The research is a part of the Project 16-05608S of the Czech Research Foundation.

REFERENCES

1. Hardwick and G. Wallwork: *Rev. High-Temp. Mater.*, 1978, vol. 4, pp. 47–74.
2. R.Prescott, M.J. Graham: *Oxid. Met.*, 1992, vol. 38, pp. 73–87.
3. P.F. Tortorelli and J.H. De Van: *Mater. Sci. Eng. A*, 1992, vol. 153, pp. 573–77.
4. N.S. Stoloff: *Mater. Sci. Eng. A*, 1998, vol. 258, pp. 1–14.
5. V.K. Sikka, D. Wilkening, J. Libertau, and B. Mackey: *Mater. Sci. Eng. A*, 1998, vol. 258, pp. 229–35.
6. C.G. McKamey, in *Physical Metallurgy and Processing of Intermetallic Compounds*, N.S. Stoloff and V.K. Sikka, eds., Chapman & Hall, New York, 1996, p. 351.
7. D.G. Morris and M.A. Munoz-Morris: *Adv. Eng. Mater.*, 2011, vol. 13, pp. 43–47.
8. M. Palm: *Intermetallics*, 2005, vol. 13 (12), pp. 1286–95.
9. D.G. Morris: *Intermetallics*, 1998, vol. 6, pp. 753–58.
10. K. Vedula, in *Intermetallic Compounds, Practice*, J.H. Westbrook and R.L. Fleischer, eds., Wiley, Chichester, 1995, Vol. 2, p. 199.
11. M.G. Mendiratta: *Mater. Res. Soc. Symp. Proc.*, 1987, vol. 81, pp. 393–404.
12. P. Kratochvíl, J. Pešička, R. Král, M. Švec, and M. Palm: *Metall. Mater. Trans. A*, 2015, vol. 46A, pp. 5091–94.
13. R.L. Fleischer: *Acta Metall.*, 1963, vol. 11, pp. 203–09.
14. R. Labusch: *Phys. Status Solidi (B)*, 1970, vol. 41b, pp. 659–69.
15. D.G. Morris and M.A. Munoz-Morris: *Intermetallics*, 2005, vol. 13, pp. 1269–74.
16. G. Hasemann, J.H. Schneibel, and E.P. George: *Intermetallics*, 2012, vol. 21, pp. 56–61.
17. F. Stein, A. Schneider, and G. Frommeyer: *Intermetallics*, 2003, vol. 11, pp. 71–82.
18. F. Stein, MPIE Stuttgart, Germany, unpublished research, 2017.
19. L. Anthony and B. Fultz: *Acta Metall. Mater.*, 1995, vol. 43, pp. 3885–91.
20. M. Palm, G. Inden, and N. Thomas: *J. Phase Equilib.*, 1995, vol. 16, pp. 209–22.
21. I. Ohnuma, C.G. Schön, R. Kainuma, G. Inden, and K. Ishida: *Acta Mater.*, 1998, vol. 46, pp. 2083–93.
22. A. Michalčová, L. Senčková, G. Rolink, A. Weisheit, J. Pešička, M. Stobik, and M. Palm: *Mater. Des.*, 2017, vol. 116, pp. 481–94.